

44p.  
final report

Contract No. NAS5-3142

30 August 1963

RSI SATELLITE COMMAND  
ANTENNA ARRAY  
Model 071-024

VOLUME I - ELECTRICAL

Prepared for:

National Aeronautics and Space  
Administration - Goddard Space  
Flight Center, Greenbelt, Md.

Prepared by:

R. W. Hurlburt, Jr.  
R. W. Hurlburt, Jr., Project Engineer

Approved by:

G. G. Chadwick  
G. G. Chadwick, Sr. Staff Engineer

OTS PRICE

XEROX

\$

4.60 ph

MICROFILM

\$

1.52 mf

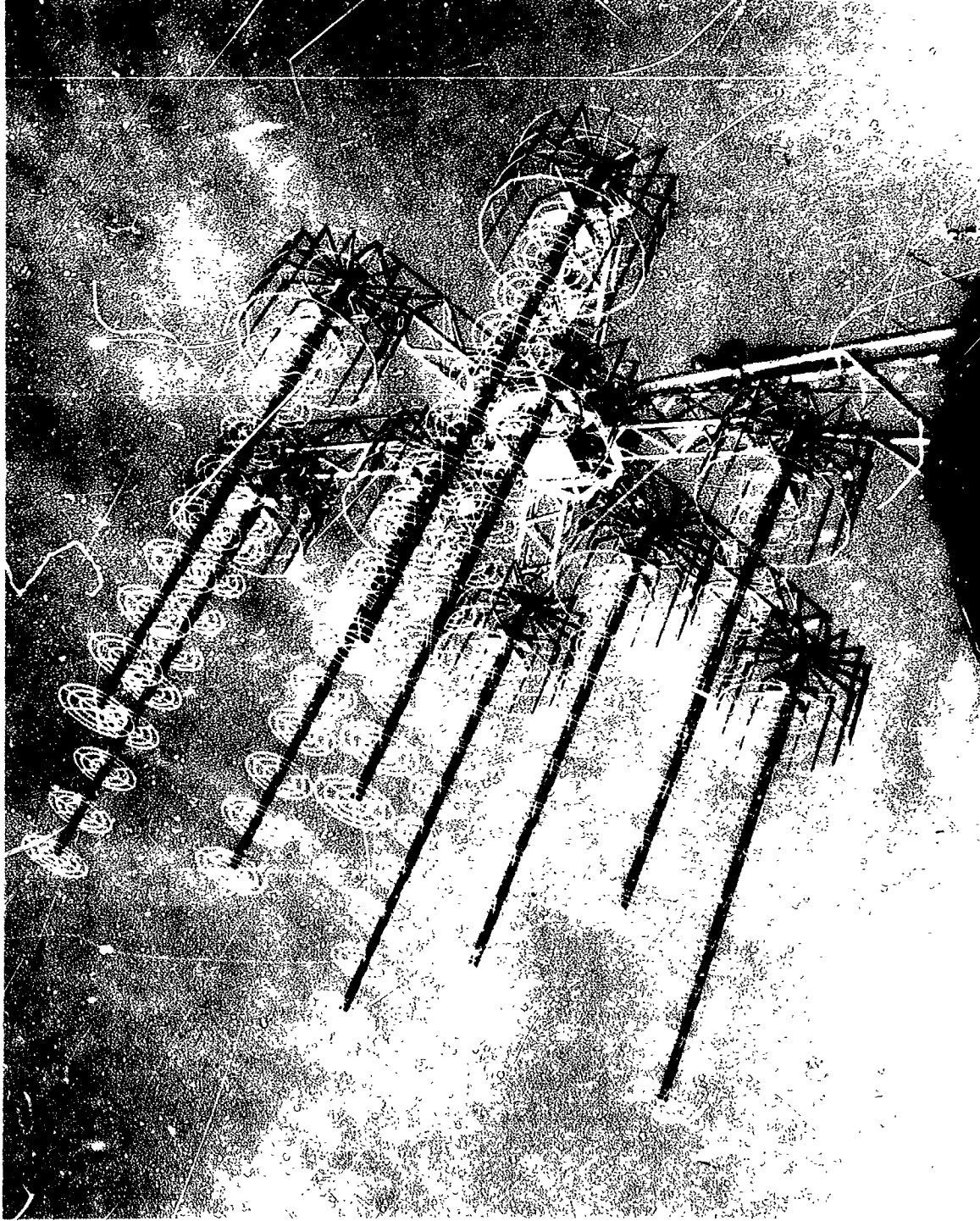


Figure 1. RSi Satellite Command Antenna Array

## TABLE OF CONTENTS

	<u>Page</u>
1.0 INTRODUCTION	1
2.0 SPECIFICATIONS	1
3.0 GENERAL DESCRIPTION AND DESIGN APPROACH	1
4.0 DISC-ON-ROD ELEMENTS	6
5.0 NINE-WAY POWER DIVIDER	10
6.0 POLARIZATION CONTROL	15
7.0 TEST RESULTS	17
7.1 Measurement Procedures	17
7.1.1 Voltage Standing Wave Ratio	17
7.1.2 Radiation Patterns	17
7.1.3 Gain Measurements	17
7.2 Array - Serial Number One	25
7.3 Array - Serial Number Two	26
7.4 Array - Serial Number Three	26
7.5 Array - Serial Number Four	27
8.0 RECOMMENDATIONS AND CONCLUSIONS	27

## LIST OF ILLUSTRATIONS

	<u>Page</u>
Figure 1. RSi Satellite Command Antenna	Front Page
Figure 2. Nine-element Array Configuration	3
Figure 3. Computed Array Patterns at 120 mc	4
Figure 4. Computed Array Patterns at 150 mc	5
Figure 5. Scale Model Three-element Array	7
Figure 6. Gain vs. Number of Elements - 4.5 Scale Model	8
Figure 7. Typical Single Element Performance.	9
Figure 8. Design of the Nine-way Power Divider.	11
Figure 9. Average Power Capacity as a Function of the Outer Dielectric Diameter for Teflon-loaded Coaxial Cable.	12
Figure 10. VSWR of Nine-way Power Divider	13
Figure 11. Nine-way Power Divider Units	14
Figure 12. Feed Network.	16
Figure 13. Polarization Control Panel with Polarization Box.	18
Figure 14. Polarization Box Interior.	19
Figure 15. Typical 3-db Coupler Performance.	20
Figure 16. VSWR Test Set-up.	21
Figure 17. Array Erected on Roof for VSWR Measurements.	22
Figure 18. Set-up For Gain Measurement by Transmission Method.	24

## 1.0 INTRODUCTION

This final report has been prepared in accordance with NASA Contract No. NAS5-3142, Article V, Paragraph B. This report has been subdivided into two volumes. Volume I is concerned with the electrical design considerations, final test data and a section of recommendations and conclusions. Volume II covers the mechanical calculations which were necessary for the design of the subject arrays.

## 2.0 SPECIFICATIONS

Table 1-1 describes the electrical specifications of the RSi Satellite Command Antenna Array, Model No. 071-024.

TABLE 1-1

### Electrical Specifications

Frequency range:	120 - 155 mc
Gain:	22 db
Input impedance:	50 ohms
VSWR (at 122.9, 148.26, 148.56 and 148.98 mc):	max. 1.20
Average power:	7.5 kw
Sidelobe level:	-13 db
Backlobe level:	-25 db
Beamwidth:	Not specified
Polarization modes:	Parallel Y-axis, perpendicular Y-axis, right-hand circular, left-hand circular.

## 3.0 GENERAL DESCRIPTION AND DESIGN APPROACH

The RSi Satellite Command Antenna Array design has remained basically the same as described in RSi's technical proposal dated 21 January 1963. The array consists of nine (9) disc-on-rod antenna elements, each capable of radiating in either of two linear orthogonal polarization modes. These antenna elements are excited by two high-power, nine-way power dividers. One power divider excites the vertically polarized inputs of the disc-on-rod elements and the other power divider excites the horizontally polarized inputs. The two inputs of these power dividers are processed through a polarization control network which allows the remote selection of horizontal, vertical, circular left- and circular right-hand polarization. All of the above subcomponents, except the

remote control panel are mounted on the array support structure. The remote control panel, designed to fit a 19-inch rack, will be located in the main equipment console.

The element orientation is illustrated in Figure 2. The arrangement was generated by using a series of three isosceles triangles all having a common center. The innermost and outermost element trios are located on the corners of two isosceles triangles with the apex of the triangles directed towards the top of the sheet. The intermediate trio of elements are located on the corners of a third triangle with the apex directed to the bottom of the page. The basic interelement spacing is set at one wavelength at 121 mc (8.12 feet). This array configuration was examined by utilizing experimentally derived disc-on-rod element patterns in conjunction with simple array theory. The element pattern characteristics used in the computations are listed below.

Frequency:	120 mcs	150 mcs
Absolute gain:	11.7 db	12.2 db
Half-power beamwidth:	43°	40°
First sidelobe level:	-17.0 db	-13.0 db

The computed patterns are shown in Figures 3 and 4 for both X and Y planes, at frequencies of 120 mcs and 150 mcs respectively. The X and Y planes of the array are defined in Figure 2. The following tabular data summarizes the computed performance of the array.

Frequency:	120 mcs	150 mcs
Absolute gain:	+20.8 db	+21.4 db
Absolute gain increase above element:	+9.1	+9.2
Half-power beamwidth:	16°	14°
First sidelobe level (ave.)	-31.0 db	-20.0 db
Major sidelobe level (ave.)	-26.0 db	-24.0 db

The absolute gain was derived by numerical integration of the computed array patterns. Examination of the tabular data will indicate that a minimum gain increase of 9.1 db was achieved with the nine-element array. It then appeared that an element gain of +13.0 db would be sufficient to achieve the desired level of performance (+22.0 db gain absolute).

An experimental scale model of the disc-on-rod element was constructed and tested to define the dimensions of the required unit. This unit was tested at scalar frequencies using a scale factor of 4.5 to 1. Radiation patterns and absolute gain measurements were taken at the scalar frequencies of 553 mcs

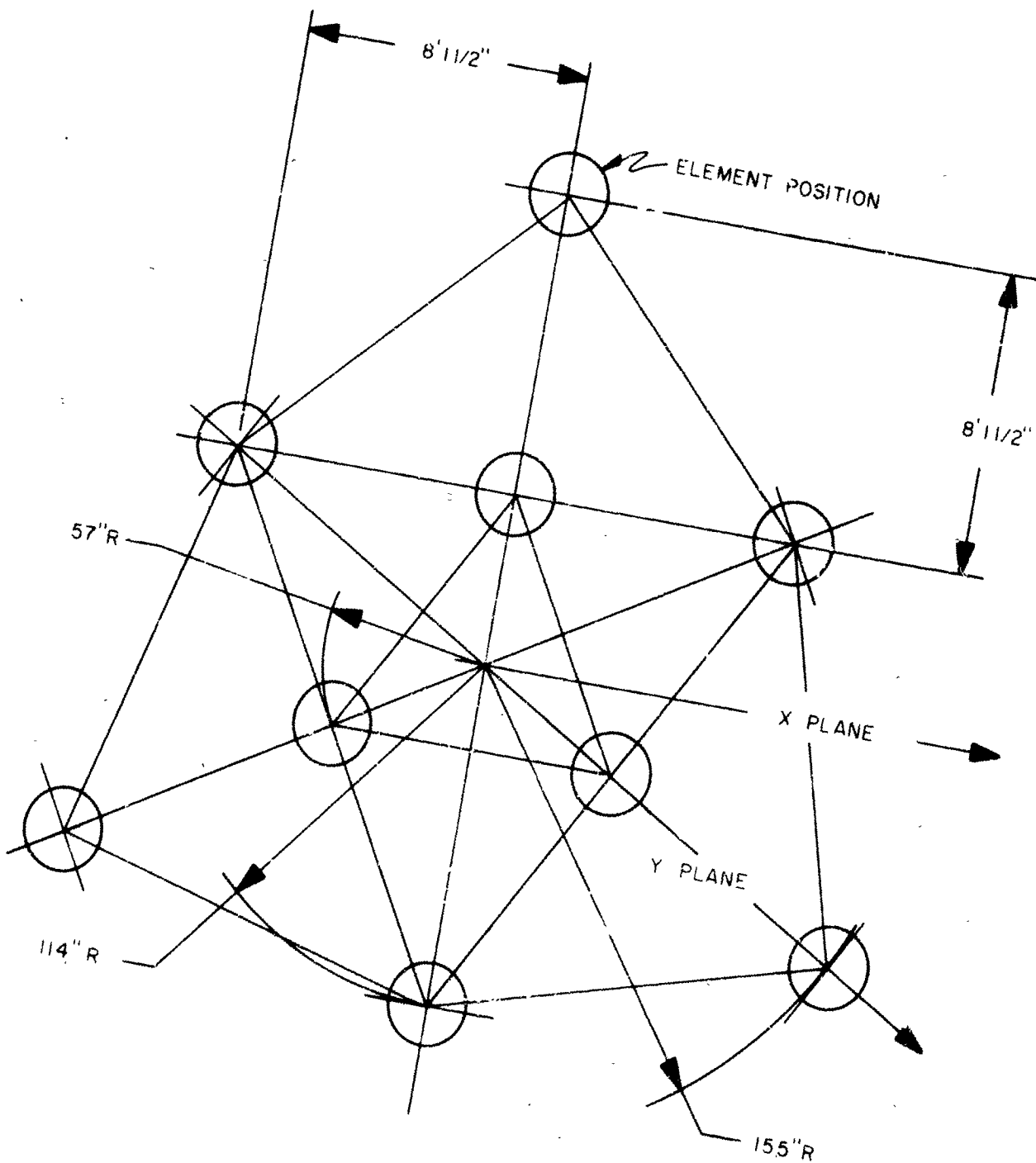


FIGURE 2 NINE-ELEMENT ARRAY CONFIGURATION

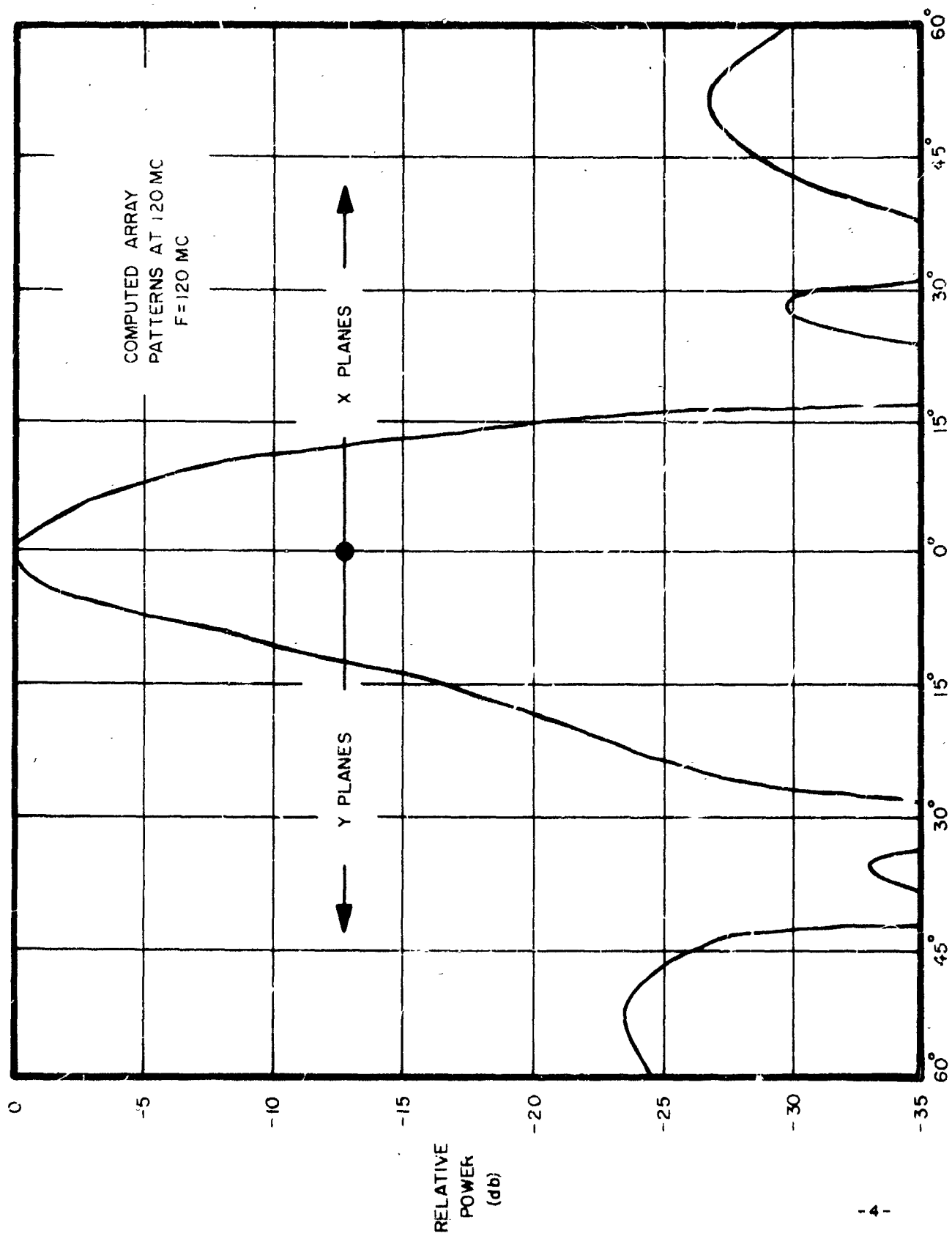


FIGURE 3.



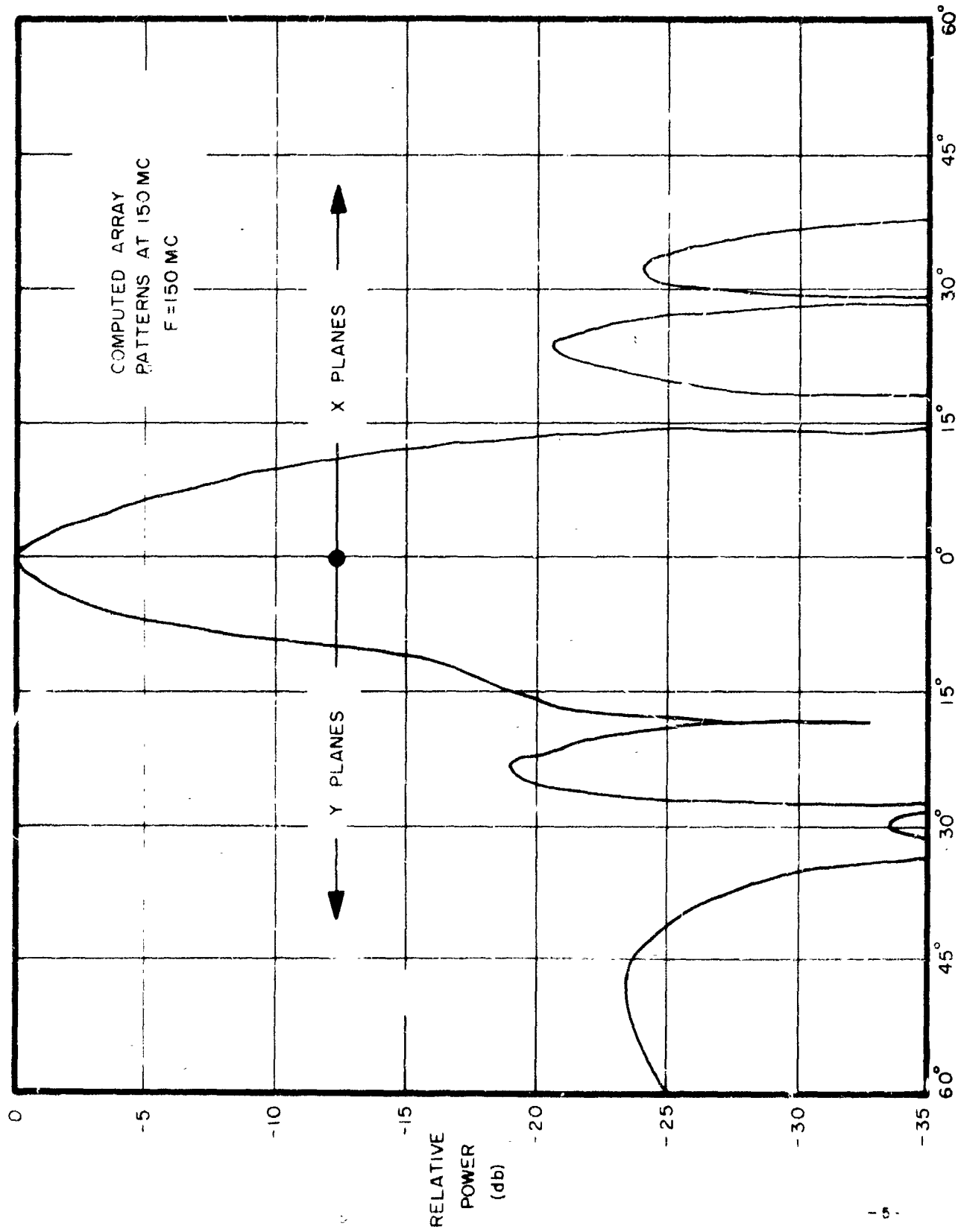


FIGURE 4

(122.9 mcs full scale) and 668 mcs (148.5 mcs full scale). The minimum element gain of +13.0 db required, as mentioned above, was achieved with this model. The first sidelobes were on the order of -13 db and the half-power beamwidths ranged from 37.5 degrees to 29 degrees. The electrical performance of this model was quite acceptable for arraying. Accordingly six of these units were arrayed and their performance evaluated.

Figure 5 is a photograph of an array of three elements which was later enlarged to a six-element array. A series of two- and three-way strip transmission line power dividers, using two-section Tchebysheff transformers allowed the array elements to be excited from a common input. A graph of gain versus number of elements is plotted in Figure 6. This data was obtained with the above mentioned scale model array by monitoring the power received while increasing the number of elements from one to six. The gain realizable from arraying these scale elements appeared sufficient to obtain the 22 db of gain for the nine-element array. The general description and design of the system subcomponents will follow in a later section of this report.

#### 4.0 DISC-ON-ROD ELEMENTS

Following the construction and testing of the scale model array, two full scale disc-on-rod elements were fabricated and tested. Radiation patterns and absolute gain measurements were taken on these units to verify the scaling factor of 4.5 to 1. These first full scale disc-on-rod elements consisted of ten discs, 31 1/2" diameter, spaced at 20". The circular cavity which serves to equalize the E- and H-plane beamwidths was 44 1/4" high and 64 1/4" diameter. The gain of these first units was not sufficient. Adjustments of disc diameter and spacing were made until the absolute minimum gain at the low end of the frequency band was 13 db, the minimum value to achieve 22 db gain with the nine-element array. Single element gain and sample patterns are shown in Figure 7. The final disc-on-rod configuration consisted of ten discs, 29 1/2" diameter, spaced at 22 1/2" with the exception of the first disc which was placed eight inches from the top of the dipole sleeve. This disc is mounted using clamps whereas the remaining discs are welded in place. The first disc has remained adjustable for use as a final matching device without effect on radiation pattern or gain performance. The cavity was not changed from its original dimensions.

With the disc-on-rod element configuration finalized, this unit was matched utilizing a series line-transformer section incorporated in the dipole coaxial feed line. A VSWR of 1.1 or less was obtainable at the desired frequencies of 122, 123, 148 and 149 mcs.

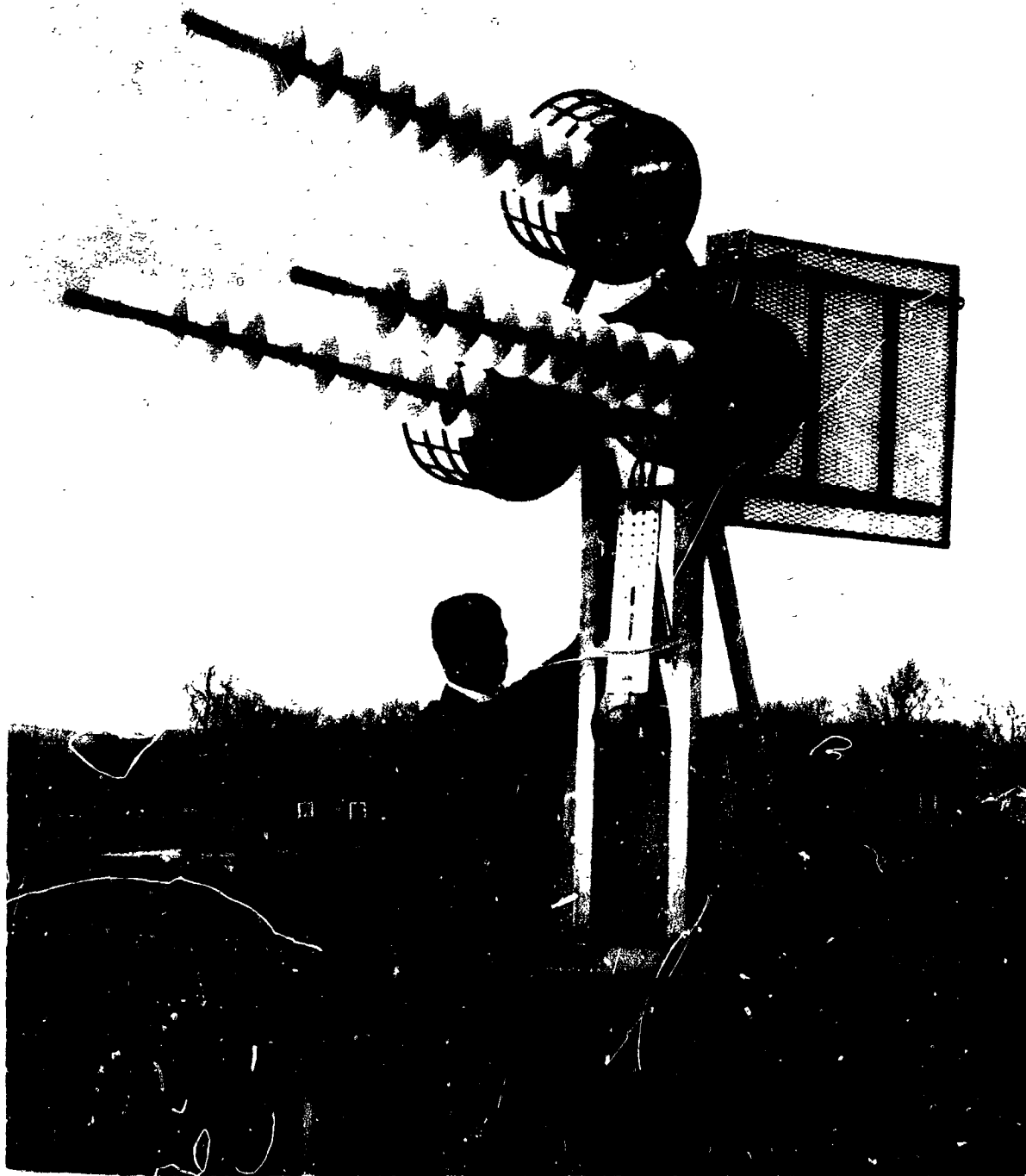


Figure 5. Scale Model Three-element Array.

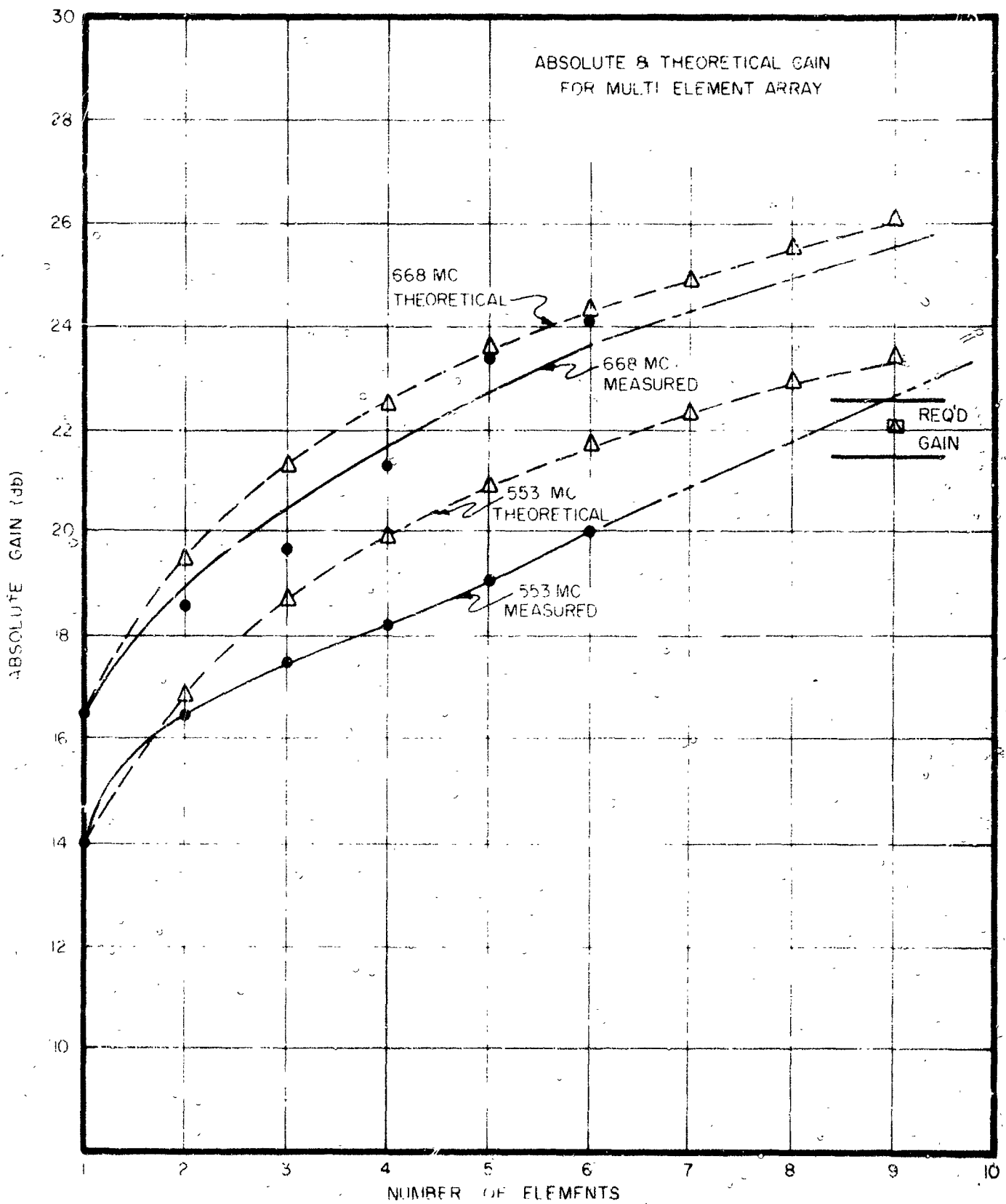
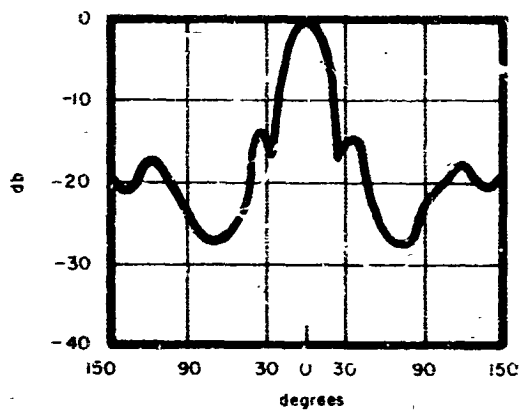
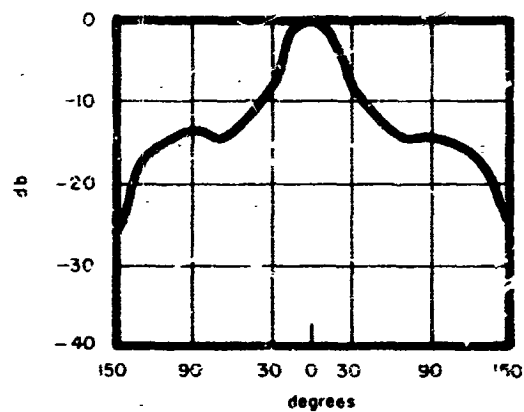


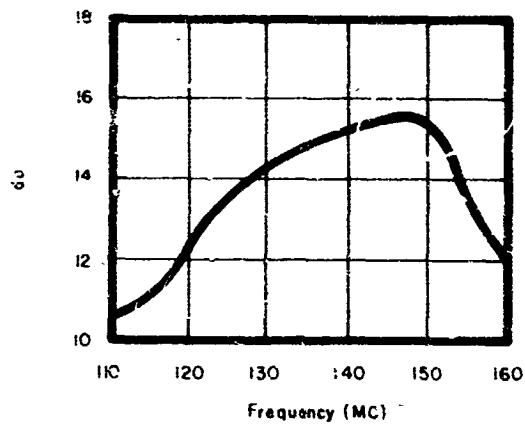
FIGURE 6 GAIN VS. NUMBER OF ELEMENTS - 4.5-SCALE MODEL



123 MC "E" PLANE



148 MC "E" PLANE



ABSOLUTE GAIN

Figure 7. Typical Single Element Performance.

## 5.0 NINE-WAY POWER DIVIDER

Two nine-way power dividers are required to implement the system. The electrical design is schematically described in the sketch of Figure 8. The unit is basically composed of four three-way power dividers interconnected by three coaxial cables. Each power divider is a two-section transformation from a single 50 ohm input to three 50 ohm outputs. The values of  $Z_1$  and  $Z_2$  are 37.7 and 22.2 ohms, respectively.

The power divider units were fabricated in strip-transmission line with teflon as the dielectric medium. A problem of some concern was the line thickness which must be used to accommodate 7.5 kw of average power in the first power divider unit. The power handling capability depends on, among other things, the heat sink available, the ambient temperature, air flow, allowable temperature rise, the materials used and the field density within the transmission line. Rather than base the design on computations made on strip-transmission lines, a more conservative approach was used. Coaxial cable, with its conservative manufacturer's power rating was selected and its dimensions were converted to strip transmission line equivalent.

Figure 9 is a plot of the average power capacity of commercial teflon dielectric cable as a function of the outer dielectric diameter, at frequency of 155 mcs. These curves were extrapolated from data available on coaxial cables listed by the Amphenol Corporation of Broadview, Illinois. Examination of the graph will indicate that a diameter of 0.430 inches is required to handle 7.5 kw of average power and a diameter of 0.220 inches would be required to handle 2.5 kw of average power. If the thickness of the strip-transmission lines were made equal or greater than these values, then the power capacity should be somewhat higher. The fact that the strip-transmission line will handle more power is due to the decreased field intensity and increased heat sink capacity of this type of line compared to coaxial cable. To further increase the safety factor, the thicknesses of 0.500 inches and 0.375 inches were used in designing the power dividers to handle 7.5 kw and 2.5 kw of average power, respectively.

In all of the power divider modules, the center conductor thickness is 1/8 inch, with radiuses of 1/16 inch. The main input connector is a modified type "L1" panel jack. The intermediate and output adaptors are modified UG-58/U panel jacks. The intermediate cabling is RG-116/U and the output cabling, from the power divider units to the dipole inputs, is RG-115A/U coaxial cable. Figure 10 is a plot of VSWR versus frequency of a nine-way power divider, and Figure 11 is a photograph of two of these units.

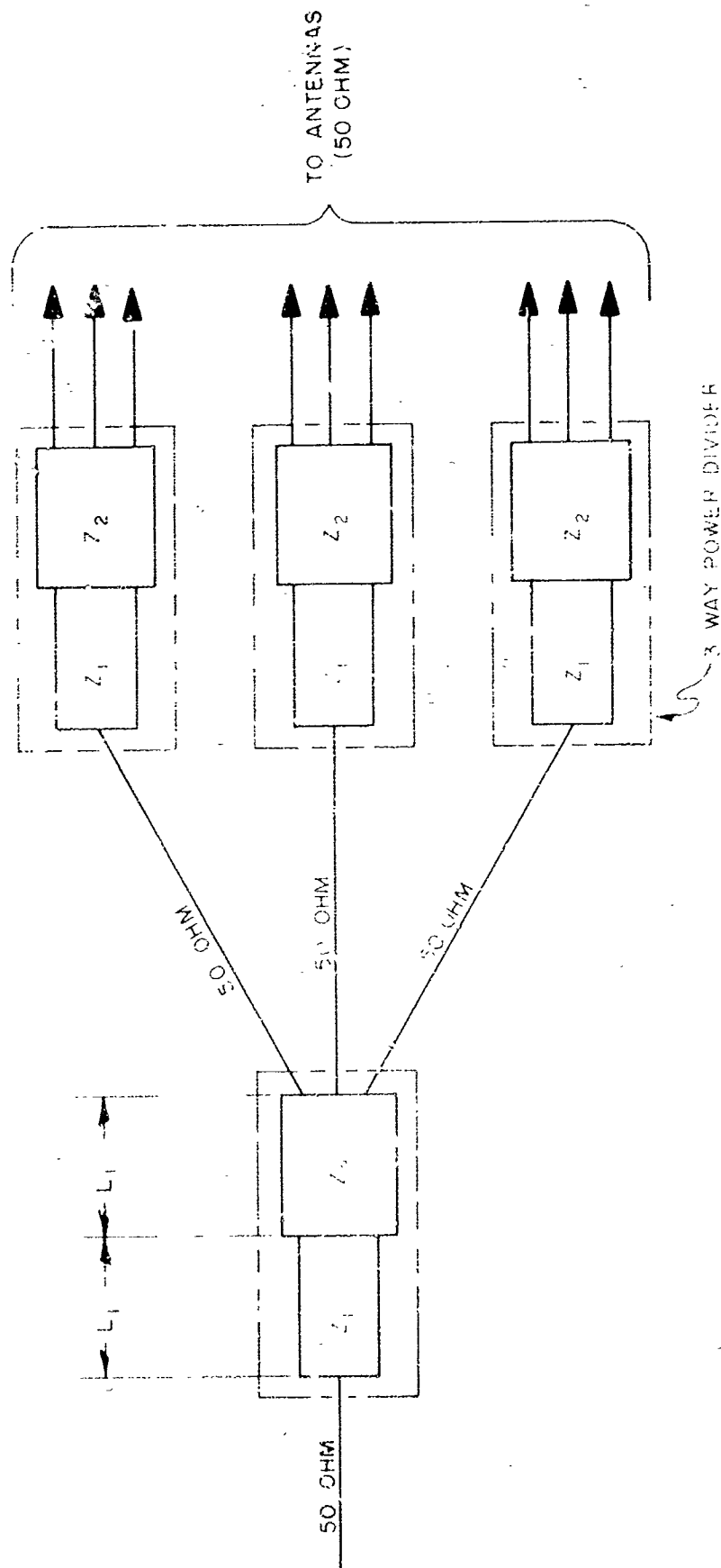


FIGURE 3 DESIGN OF THE NINE-WAY POWER DIVIDER

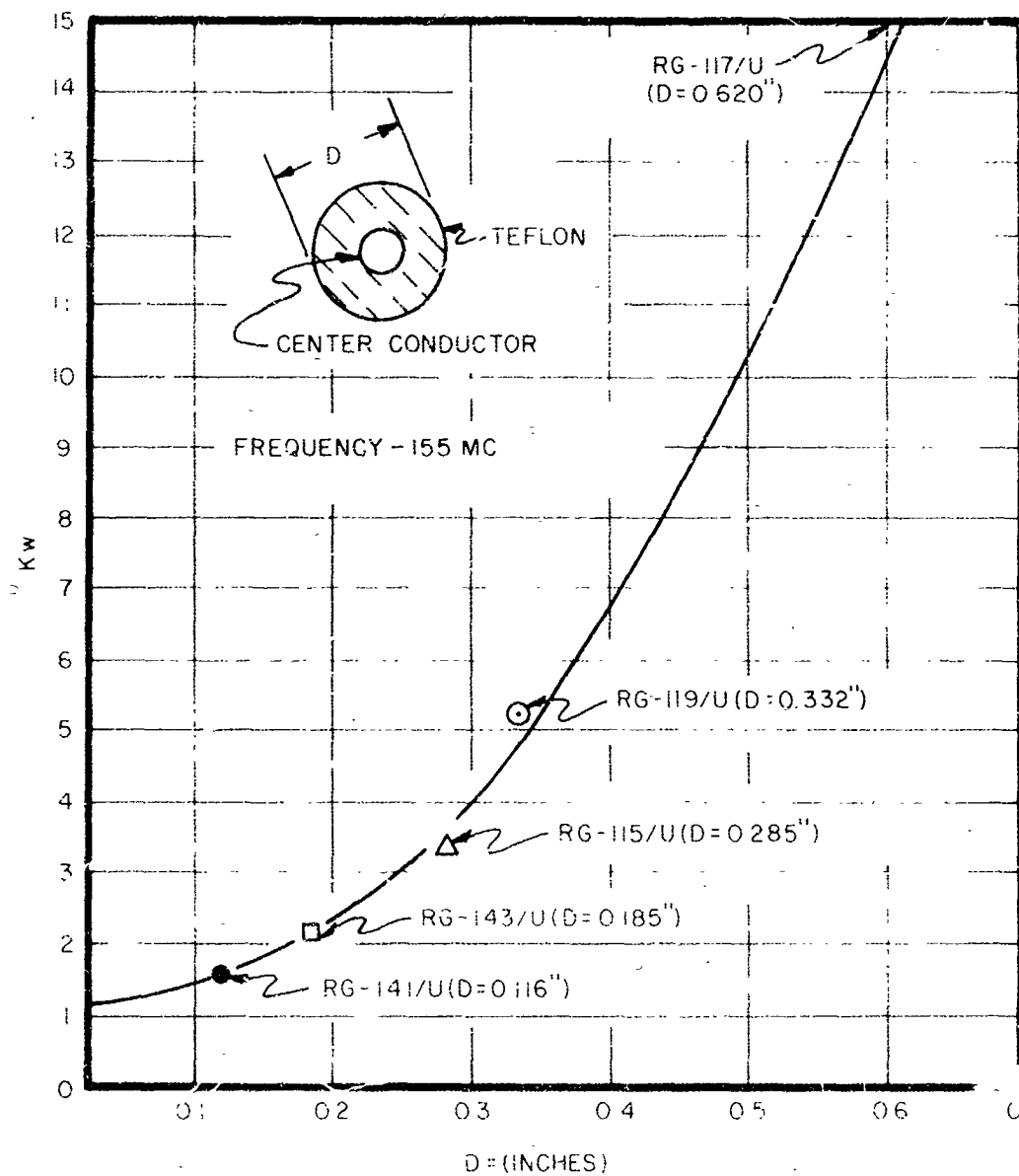


FIGURE 9 AVERAGE POWER CAPACITY AS A FUNCTION OF THE OUTER DIELECTRIC DIAMETER FOR TEFLON-LOADED COAXIAL CABLE



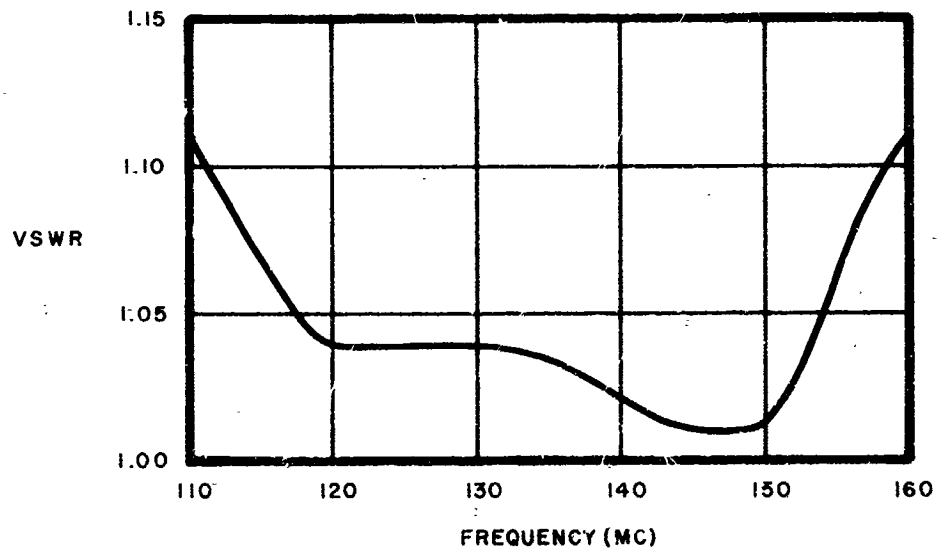


Figure 10. VSWR of Nine-way Power Divider

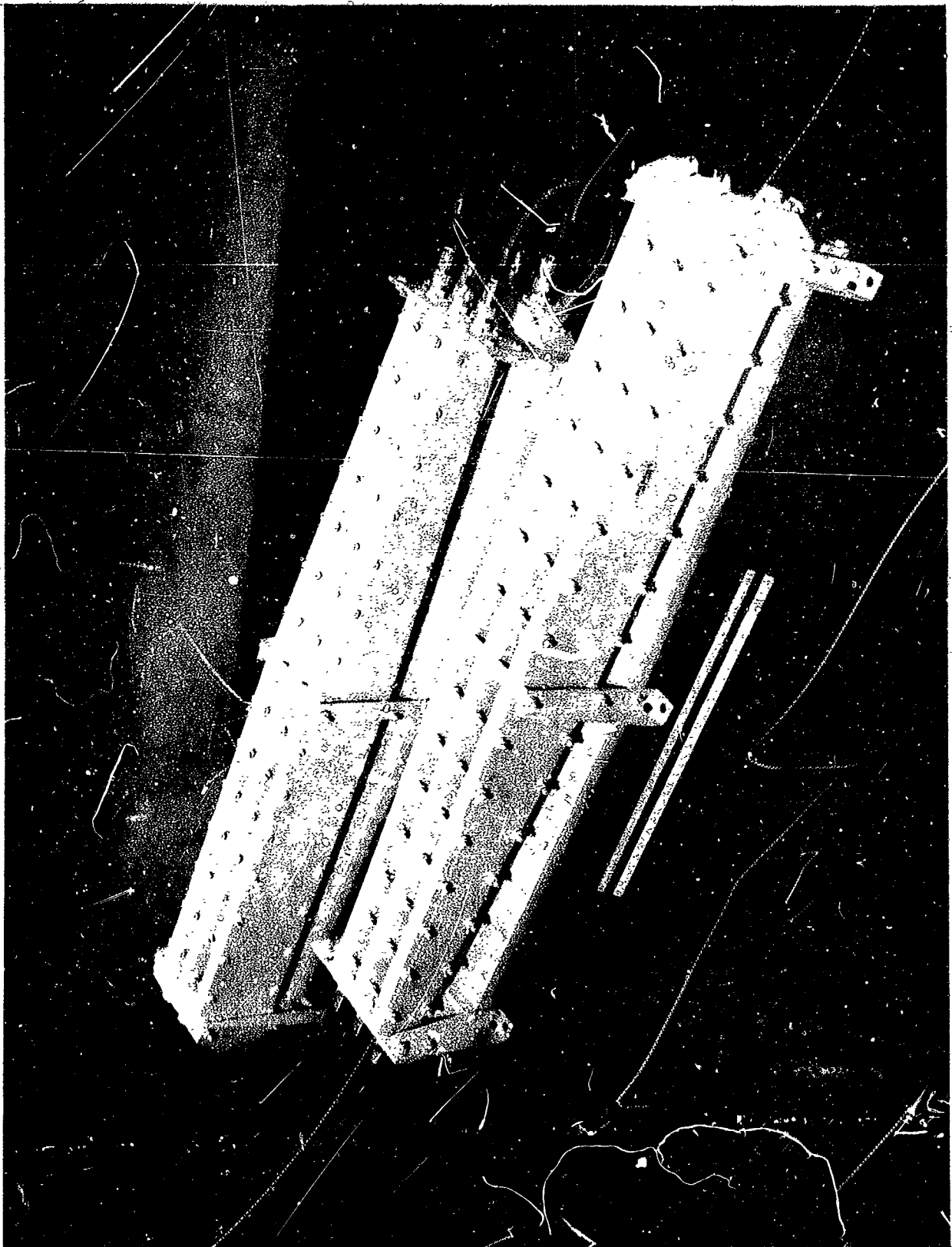


Figure 11. Nine-way Power Divider Units

## 6.0 POLARIZATION CONTROL

The feed network which processes the inputs of the two power dividers is schematically shown in Figure 12. The horizontal and vertical inputs of the two nine-way power dividers are each connected to one terminal of two SPDT switches (A and B). When switch A is connected to terminal 1 and the SP4T switch is connected to terminal //Y, the input polarization is parallel to the Y axis. Correspondingly, when switch B is connected to terminal 4 and the SP4T switch is connected to terminal  $\perp$ Y, the input polarization is perpendicular to the Y axis. To excite either sense of circular polarization, switches A and B are connected to terminals 2 and 3 respectively. These ports are connected to the two output arms of the 3-dB coupler. A signal at arm 2 causes a voltage equal to  $-0.707 E_{//Y}$  to appear at one input to the coupler (5). In addition, a voltage equal to  $-j0.707 E_{//Y}$  will appear at the second hybrid input. In the same manner a signal at terminal 3 excites a voltage of  $-j0.707 E_Y$  at port 5, and  $0.707 E_Y$  at port 6. Thus, the sum of the voltages at port 5 of the hybrid is equal to

$$E_5 \approx 0.707 E_{//Y} - j0.707 E_{\perp Y},$$

which is the condition for left-hand circular polarization. The total voltage appearing at terminal 6 is of the form

$$E_6 \approx 0.707 E_{\perp Y} - j0.707 E_{//Y},$$

which is the condition for right-hand circular polarization. The input polarization is now controlled by the position of the SP4T switch. The performance of the network can be summarized as follows:

<u>Mode</u>	<u>"A" Switch Connection</u>	<u>"B" Switch Connection</u>	<u>SP4T Connection</u>
//Y	1	-	//Y
$\perp$ Y	-	4	$\perp$ Y
Left-hand circular	2	3	LC
Right-hand circular	2	3	RC

A remote control selector is used to energize the polarization switches in proper sequence. This control panel has indicator lights connected to relays in the switches. These lights give positive indication that the switches are functioning properly.

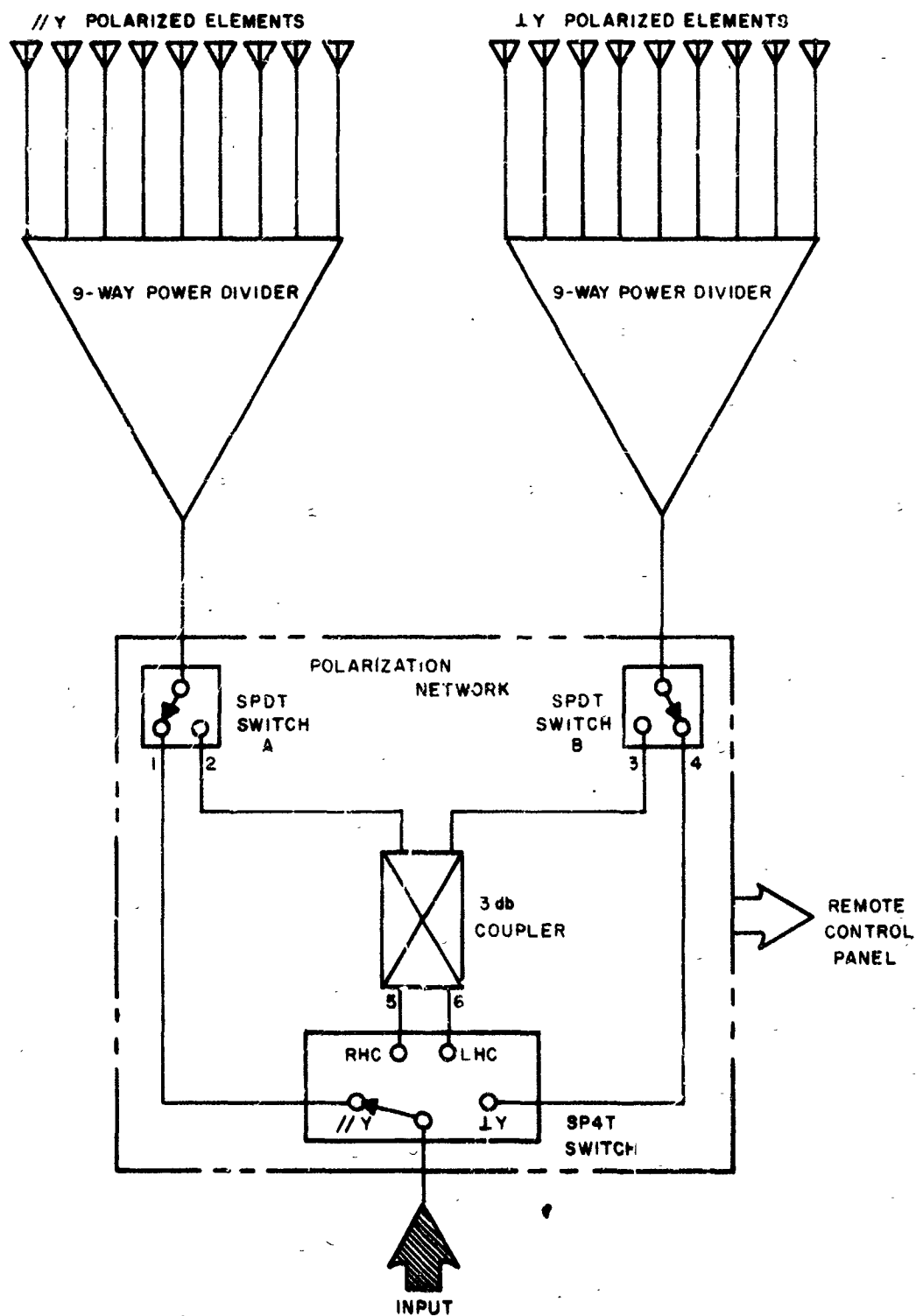


FIGURE 12. FEED NETWORK

Figure 13 is a photograph of the polarization control unit. The control unit, designed for rack mounting has the four polarization conditions: //Y, ⊥Y, left-hand circular and right-hand circular. An indicator light is provided for each position. In addition, a test switch is provided which allows each r-f coaxial switch to be examined to insure proper operation.

A photograph of the interior of the polarization unit is shown in Figure 14. It contains three high-power switches and a high-power 3-db coupler. This unit is mounted on the central hub of the array, and is completely sealed to protect its contents from the antenna environment.

Figure 15 shows the typical 3-db coupler performance.

## 7.0 TEST RESULTS

### 7.1 Measurement Procedures

7.1.1 Voltage Standing Wave Ratio - A General Radio Company type 1602-B admittance meter and associated equipment were used to determine the VSWR of the antenna system. The test setup is shown in Figure 16. Array number one was tested while mounted on the radiation pattern range, as shown in Figure 1. Arrays two, three and four were tested while erected upon the roof, as shown in Figure 17.

7.1.2 Radiation Patterns - Radiation patterns were taken as the array was rotated about the Y axis. The radiation patterns are included later in this report.

7.1.3 Gain Measurements - In Antennas by John D. Kraus<sup>1)</sup>, the following formula is given representing the ratio of received power to transmitted power of two antennas in free space:

$$\frac{W_r}{W_t} = \frac{G_r G_o \lambda^2}{(4\pi r)^2}$$

where  $W_r$  = received power  
 $W_t$  = transmitted power

---

1. John D. Kraus, "Antennas," Ph. D., the Ohio State University, McGraw-Hill Book Company; 1950.

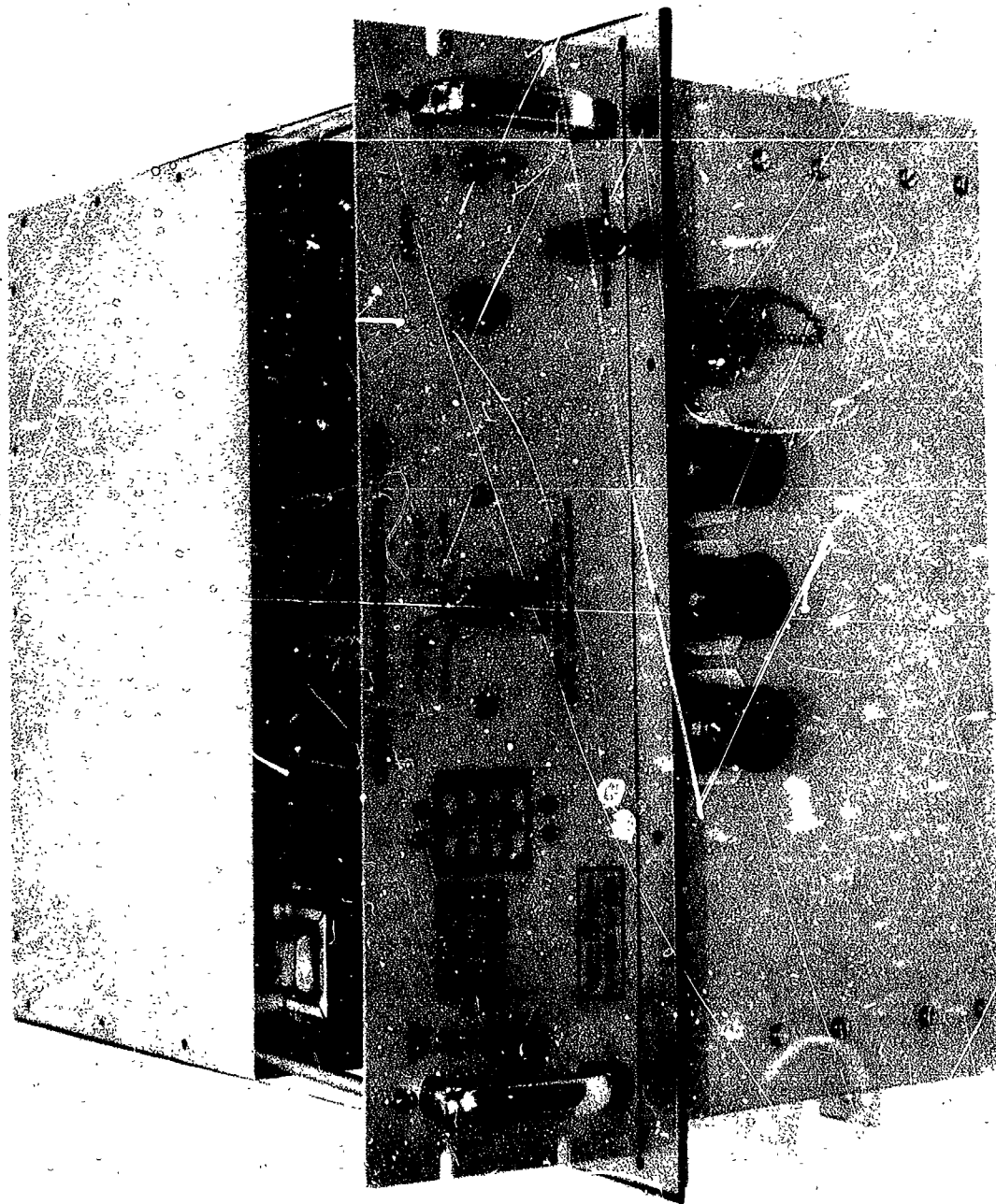


Figure 13. Polarization Control Panel with Polarization Box.

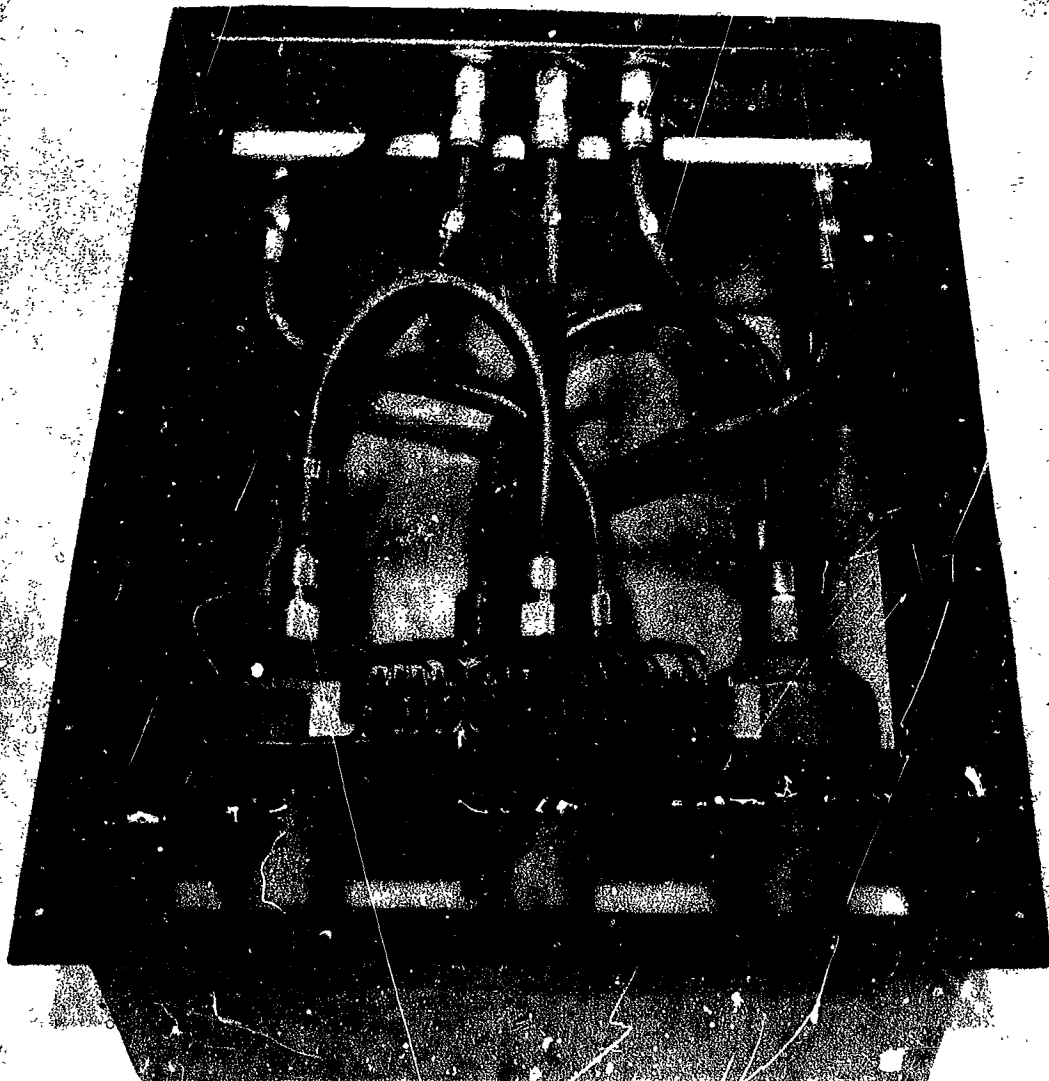
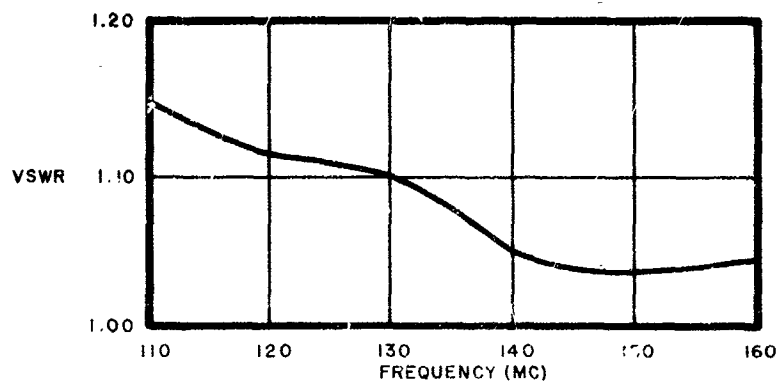
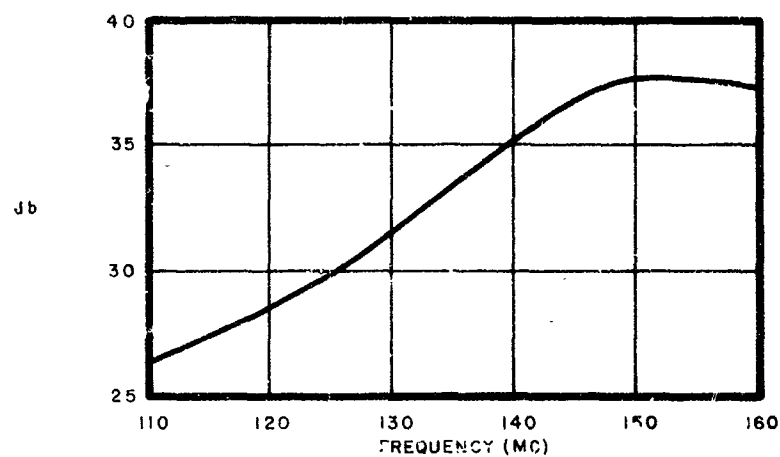


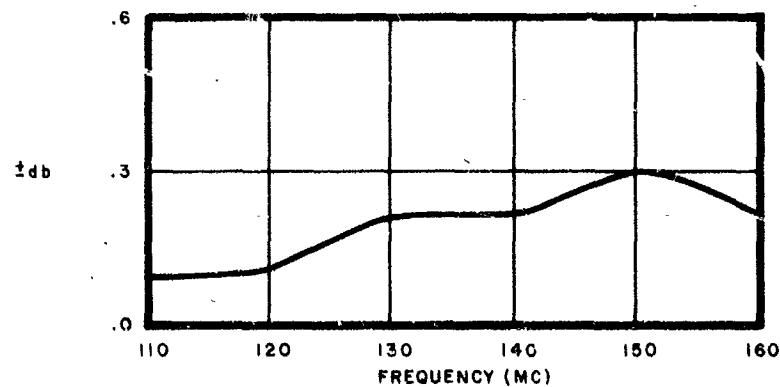
Figure 14. Polarization Box Interior



VSWR



ISOLATION



COUPLING UNBALANCE

Figure 15. Typical 3-db Coupler Performance.



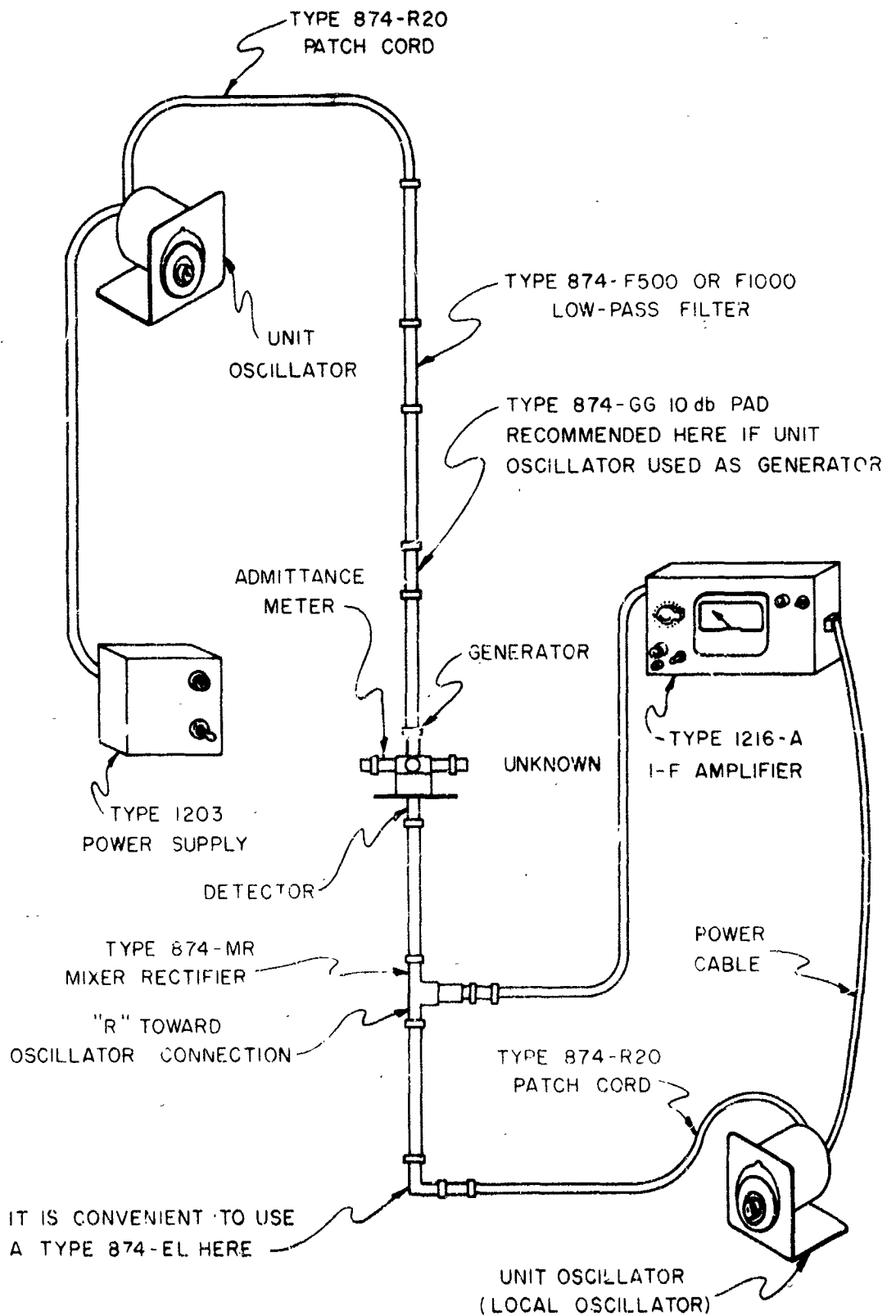


FIGURE 16. VSWR TEST SET-UP

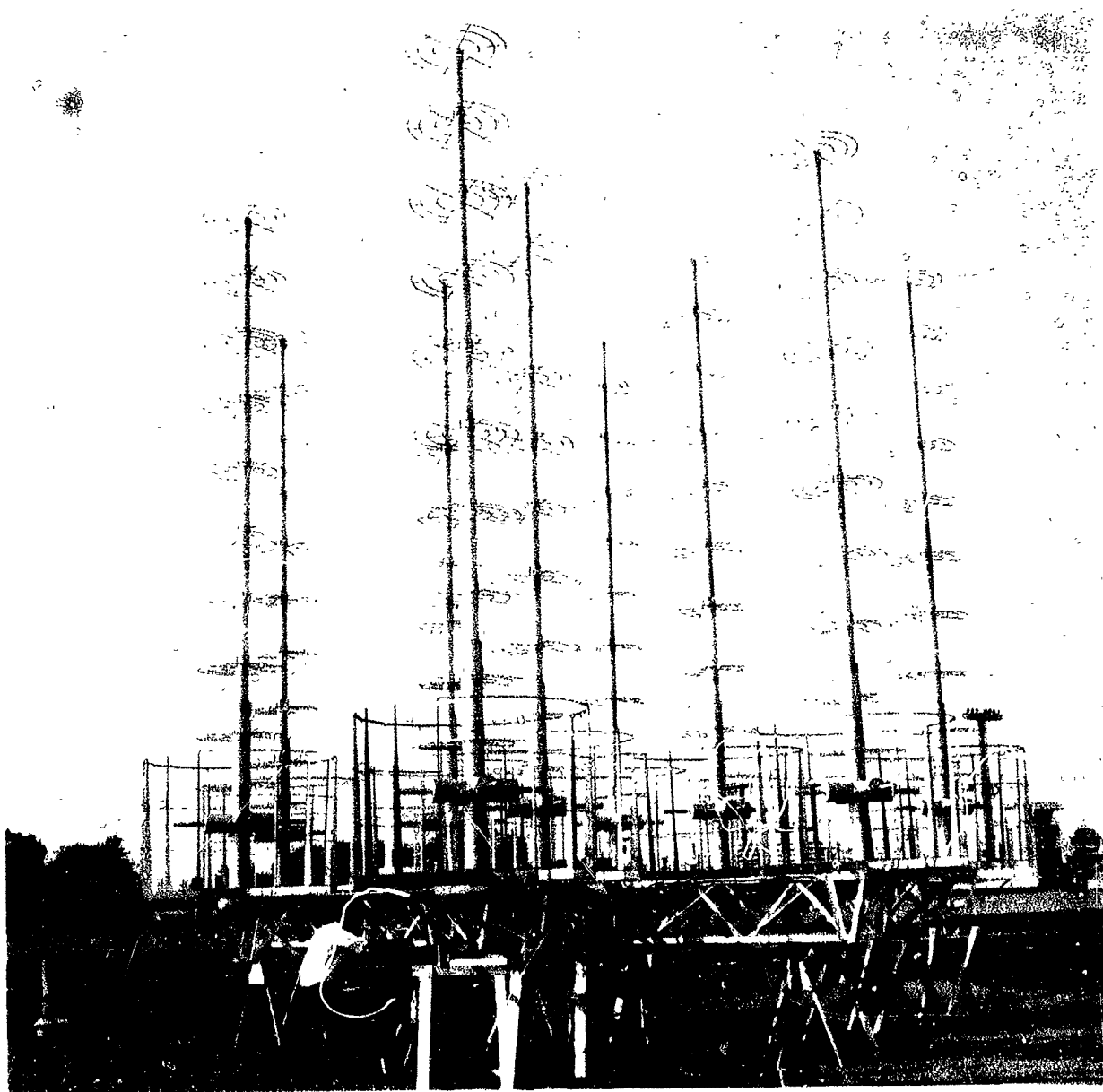


Figure 17. Array Erected on Roof for VSWR Measurements.

$\lambda$  = free space wavelength  
 $G_{or}$  = gain of receiving antenna over an isotropic source.  
 $G_{ot}$  = gain of transmitting antenna over an isotropic source.  
 $r$  = distance between antennas.

Converting this formula to a decibel relationship, we get

$$G_r + G_t = 20 \log \left( \frac{4\pi r}{\lambda} \right) + 10 \log \left( \frac{W_r}{W_t} \right),$$

where  $G_r$  = gain of receiving antenna expressed in db.  
 $G_t$  = gain of transmitting antenna expressed in db.

With  $r$  and  $\lambda$  fixed during the measurements and with a receiving antenna of known gain only two terms of this operation are unknown,  $G_t$  and  $10 \log W_r/W_t$ .

Figure 18 illustrates the test setup used to directly measure the quantity  $10 \log (W_r/W_t)$ . The above equation is then solved for  $G_t$ . The transmitting antenna in this case was the RSi Model 071 Satellite Command Antenna array and the receiving antenna was a single disc-on-rod element identical to the units incorporated in the array. This latter unit had been calibrated using the identical antenna method with the above formula.

With  $r$  and  $\lambda$  fixed,  $10 \log (W_r/W_t)$  can be measured directly. Then the equation is solved for  $G_t + G_r = 2G$ . As a check of this method, three identical antennas were used. The results were within normal reading error.

To check the transmission method of gain measurements, the radiation patterns were numerically integrated. The directivity,  $D$ , of an antenna is stated in Antennas by Kraus to be

$$D = \frac{4\pi (\text{maximum radiation intensity})}{\text{Total power radiated}}$$

If it is assumed that a radiation pattern plotted in relative power is symmetrical about the axis of maximum radiation and the maximum power is set equal to 1, then the total power radiated can be represented by the integral,

$$\int_0^{2\pi} \int_0^{2\pi} P(\theta) \sin \theta \, d\theta \, d\phi$$

where  $P(\theta)$  is relative power at some azimuth angle  $\theta$   
 $\phi$  is elevation angle.

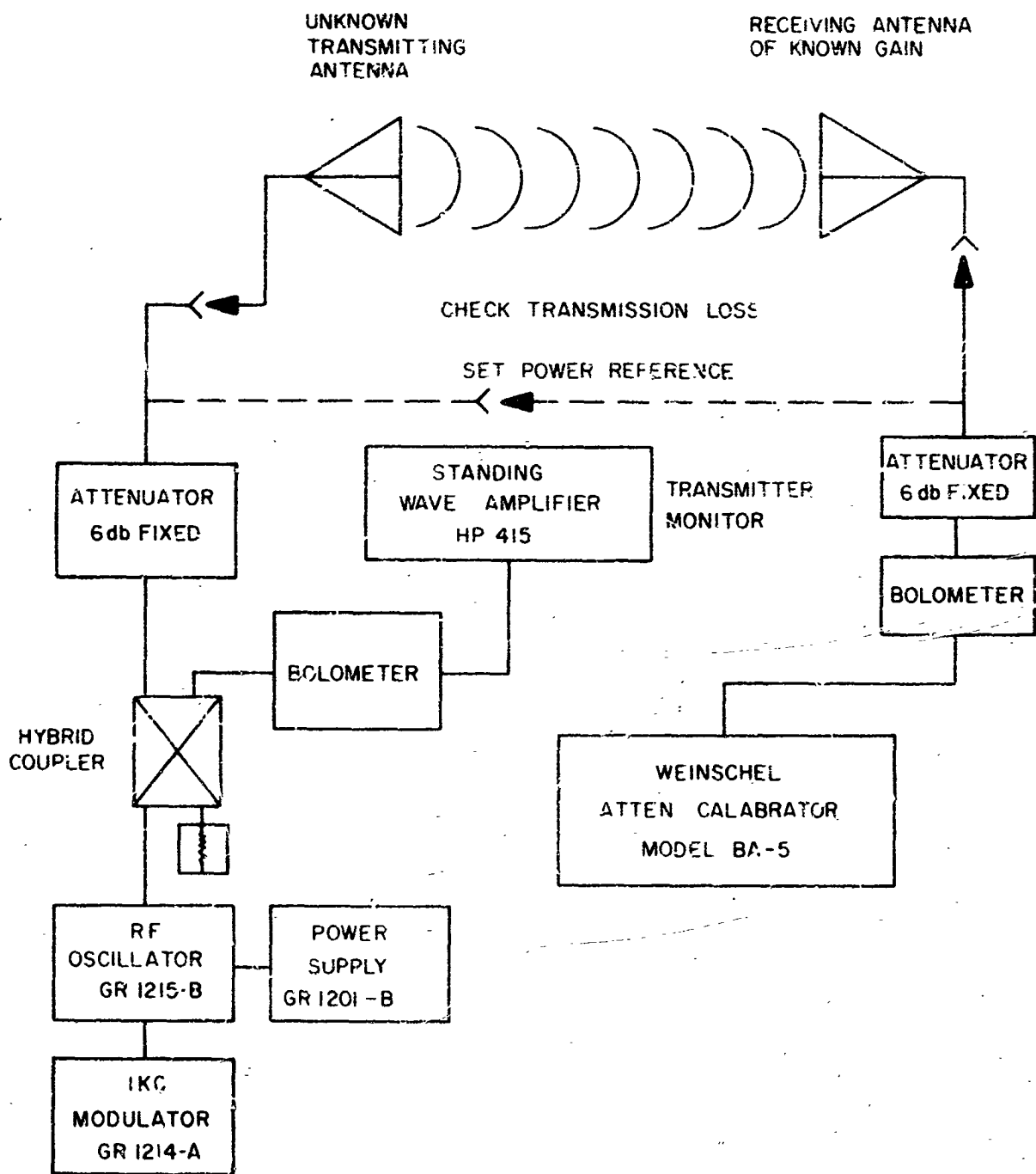


FIGURE 18. SET-UP FOR GAIN MEASUREMENT BY TRANSMISSION METHOD.

The integral

$$\int_0^{\pi} P(\theta) \sin \theta d\theta$$

can be solved by determining the area under the curve representing  $\sin \theta$  times the relative power at each azimuth angle,  $\theta$ , from 0 to  $\pi$ . The area can be found by numerically summing the areas of small rectangular increments under the curve, each with a width of  $b$  radians and a height of  $P(\theta) \sin \theta$ . The outer integral,

$$\int_0^{2\pi} f(\theta) d\theta$$

is equal to  $2\pi$ .

The directivity can therefore be written

$$D = \frac{4\pi}{2\pi (b \text{ radians}) \left( \sum_{\theta=0}^{\pi} [P(\theta) \sin \theta] \right)}$$

Since the RSi Satellite Command Array is a direct radiating antenna, the radiation efficiency factor is very near unity and the gain is therefore very nearly equal to the directivity of the array.

Radiation patterns were not taken in a plane parallel to the Y axis because of the problems involved in handling an antenna of this size. However, computed array patterns indicate that the degree of asymmetry will not seriously compromise the accuracy of the pattern integration method of determining gain.

## 7.2 Array - Serial Number One

The following are the test results obtained with RSi Satellite Command Antenna Model 071-024, Serial Number One.

<u>Frequency (mc)</u>	<u>VSWR</u>			
	<u>//Y</u>	<u>⊥Y</u>	<u>RHC</u>	<u>LHC</u>
120	1.06	1.04	1.09	1.10
123	1.18	1.08	1.10	1.12
130	1.10	1.13	1.10	1.12
140	1.70	1.65	1.19	1.12
148	1.01	1.05	1.13	1.12
149	1.22	1.22	1.15	1.09
155	1.60	1.70	1.22	1.40

<u>Frequency (mc)</u>	<u>Average Gain*</u>
123	22.5
148	23.7

\*The average gain as measured using the two techniques described in Section 7.1.3 of this report.

The following Figures 20 through 31 are far-field radiation patterns of the array.

### 7.3 Array - Serial Number 2

The results of the VSWR measurements on the RSi Satellite Command Antenna, Model 071-024, Serial Number 2 are tabulated below:

<u>Frequency (mc)</u>	<u>VSWR</u>			
	<u>//Y</u>	<u>LY</u>	<u>RHC</u>	<u>LHC</u>
120	1.29	1.12	1.16	1.15
123	1.17	1.07	1.16	1.16
130	1.27	1.25	1.09	1.13
140	1.60	1.63	1.33	1.36
148	1.22	1.04	1.08	1.12
149	1.16	1.16	1.08	1.13
150	1.58	1.35	1.11	1.04

### 7.4 Array - Serial Number 3

The results of the VSWR measurements on the RSi Satellite Command Antenna, Model 071-024, Serial Number 3 are tabulated below. It may be noted that there are no readings for the two circular polarized modes. This was due to the lack of the required high-power switches necessary to excite these modes of operation. Prior VSWR measurements of array, Serial No. 1, indicated only a nominal change when the polarization box, which includes the switches, was removed. The data shown below is equal to, or better than, that obtained on array Serial No. 1 less the polarization box and, therefore, judged to be acceptable.

<u>Frequency (mc)</u>	<u>VSWR</u>	
	<u>//Y</u>	<u>LY</u>
120	1.04	1.10
123	1.05	1.08
130	1.20	1.13

<u>Frequency (mc)</u>	<u>VSWR</u>	
	<u>//Y</u>	<u>⊥Y</u>
140	1.44	1.45
148	1.18	1.08
149	1.27	1.11
150	1.35	1.29

#### 7.5 Array - Serial Number 4

The results of the VSWR measurements on the RSi Satellite Command Antenna, Model 071-024, Serial No. 4 are tabulated below.

<u>Frequency (mc)</u>	<u>VSWR</u>			
	<u>//Y</u>	<u>⊥Y</u>	<u>RHC</u>	<u>LHC</u>
120	1.03	1.03	1.09	1.11
123	1.16	1.16	1.16	1.09
130	1.31	1.29	1.08	1.09
140	1.62	1.50	1.21	1.28
148	1.10	1.08	1.08	1.09
149	1.21	1.21	1.08	1.10
150	1.43	1.42	1.17	1.20

#### 8.0 RECOMMENDATIONS AND CONCLUSIONS

This report has described the electrical considerations used in the design of the RSi Satellite Command Antenna Array, Model Number 071-024. Four of these arrays were designed, fabricated and delivered within six months after receipt of the order, and met the specifications given in Section 2.0.

The disc-on-rod array, in its present state or modified to meet other electrical and mechanical requirements, has many advantages over a parabolic reflector. For example, in this program, if a parabolic reflector had been used, the reflector would have been on the order of 43 feet in diameter. In addition the wind and ice loading on this structure would be significantly greater due to the low cross section of the array. The resulting requirements on the associated pedestal is thereby correspondingly reduced.

The basic nine-element array can easily be adapted to use as a monopulse tracking system. This modification would involve replacing the present polarization box with an interchangeable box containing the necessary r-f hybrids and

74978

phase shifters. Thus, by the addition of an r-f processing box and receivers, the antenna and pedestal can be converted into a self-contained precision tracking system.

It should be noted that by using the basic array configuration, i.e. elements located at the corners of isosceles triangles, the number of elements could be either increased or decreased, depending on the given gain requirements. Figure 7 in Section 3.0 illustrates the gain that can be realized with different numbers of elements from one to nine.

The single disc-on-rod element is a good basic antenna that could be used in laboratory range work or field installations. It provides good gain, polarization diversity and high power handling capacity with a relatively lightweight structure. A requirement for an antenna with a higher or lower gain specification could be met using RSI's disc-on-rod element by simply adding or subtracting discs.

*author*